Two-Dimensional Precoding for 3-D Massive MIMO

Zhaocheng Wang, *Senior Member, IEEE*, Wendong Liu, Chen Qian, Sheng Chen, *Fellow, IEEE*, and Lajos Hanzo, *Fellow, IEEE*

***Abstract*—A 2-D precoding scheme is proposed for 3-D massive multiple-input multiple-output (MMIMO) systems for efficiently exploiting the 2-D antenna array of the base station. Specifically, by exploiting the Kronecker structure of the 3-D MIMO channel matrix, the transmit precoding operation is divided into elevation-domain precoding and azimuth-domain precoding. Explicitly, in contrast to the existing beamforming schemes, precoding is also performed in the vertical dimension. Consequently, the proposed scheme is capable of fully exploiting the extra degrees of freedom provided by the vertical dimension for avoiding the interuser interference to improve the attainable system performance. Compared to the conventional scheme relying on the equivalent 1-D precoding, the proposed 2-D precoding scheme offers an improved performance in severe intercell interference-contaminated environments, despite its lower complexity.**

***Index Terms*—Interuser interference, Kronecker structure, precoding, 2-D precoding, 3-D massive multiple-input multiple-output (MMIMO).**

I. Introduction

MASSIVE multiple-input multiple-output (MMIMO) arrangements have attracted considerable attention as a benefit of their potential of significantly increasing the spectral efficiency and/or the energy efficiency by relying on low-complexity linear signal processing schemes [1]–[4]. However, most studies focus on the classic uniformly-spaced linear array (ULA), which is not suitable for practical MMIMO systems relying on a large antenna array. Three-dimensional MMIMOs [5], [6], which are also often referred to as full-dimensional MIMOs, are capable of overcoming this dimensionality problem of the base station (BS), since the array size can be reduced when the elevation domain represented by the vertical dimension is also exploited. This way, 3-D MMIMOs create extra degrees of freedom for avoiding the intercell interference while achieving an improved spectral efficiency. However, given the same total number of antenna elements at the BS, 2-D uniformly spaced rectangular arrays (URA) perform worse than the ULA due to their low resolution in the elevation domain [5], and thus, either vertical beamforming or transmit precoding (TPC) has to be invoked for improving the performance of 3-D MIMO systems [7]–[9].

A pair of existing approaches, which beneficially exploit the extra degrees of freedom introduced by the 2-D antenna array, are constituted by beamforming and multiplexing. The first approach relies on performing beamforming in the elevation domain and then invokes TPC in the equivalent azimuth domain [7], [8]. The Kronecker structure of the 3-D MIMO channel matrix is exploited and based on the approximated elevation-domain steering vector, eigenbeamforming is invoked by relying on the eigenvector corresponding to the largest eigenvalue of the elevation-domain channel's correlation matrix as the beamforming vector. As the number of antennas in the elevation domain tends to infinity, the beam becomes sufficiently narrow for the interuser interference to be mitigated [9], [10], but it still cannot be completely eliminated, which degrades the overall performance.

The second approach adopts the conventional TPC algorithm [2], [3] based on the vectorial form of the 3-D MMIMO channel matrix, where the structure of 3-D MIMO channel is not exploited. This full TPC approach suffers from the drawback of a potentially excessive complexity imposed by the TPC matrix computation. Furthermore, this full TPC algorithm is only optimal for an unrealistic single-cell scenario, i.e., in the absence of intercell interference. By contrast, in hostile intercell interference-infested environments, its performance may actually be worse than that of the beamforming scheme, as will be shown in our simulation study.

Against this backdrop, in this correspondence, we propose a 2-D TPC scheme for 3-D MMIMOs for eliminating the interuser interference. In contrast to both the conventional beamforming scheme of [7], as well as to the multilayer precoding algorithm of [8] and to the existing full TPC scheme of [2] and [3], our arrangement performs precoding in both the elevation and azimuth domains based on the Kronecker structure of the 3-D MIMO channel matrix. Specifically, the extra degrees of freedom introduced by the elevation-oriented antennas are fully exploited for distinguishing the different users roaming in the cell illuminated. As a result, the interuser interference can be completely eliminated by a finite number of elevation-domain antennas. Hence, the overall system performance is significantly improved in comparison to the conventional beamforming scheme. Compared to the conventional full precoding scheme, the proposed 2-D precoding scheme is capable of significantly outperforming the former in hostile intercell interference-contaminated environments, despite its complexity. We emphasize that indeed, the Kronecker structure of the 3-D MIMO channel matrix has been exploited for conceiving efficient channel state information feedback schemes [11]–[13]. However, to the best of our knowledge, we are the first to propose this 2-D TPC scheme, which efficiently exploits the Kronecker structure of the 3-D MMIMO channel matrix to perform TPC both in the elevation and azimuth domains.

This correspondence is organized as follows. Section II discusses the downlink system model and the Kronecker structure of the 3-D MIMO channel matrix. Section III presents the proposed 2-D TPC scheme conceived for 3-D MMIMOs, including the detailed mathematical analysis of its efficiency. Our simulation results are provided in Section IV for demonstrating the superior performance of this 2-D precoding scheme over the existing beamforming and full TPC approaches. Our concluding remarks are offered in Section V.

Manuscript received September 11, 2015; revised March 19, 2016, June 19, 2016, and September 10, 2016; accepted October 22, 2016. Date of publication October 26, 2016; date of current version June 16, 2017. This work was supported by the National Key Basic Research Program of China under Grant 2013CB329203, the National Nature Science Foundation of China under Grant 61571267, the Beijing Natural Science Foundation under Grant 4142027, the National High Technology Research and Development Program of China under Grant 2014AA01A704, the Shenzhen Visible Light Communication System Key Laboratory under Grant ZDSYS20140512114229398, and the Shenzhen Peacock Plan under Grant 1108170036003286. The review of this paper was coordinated by Prof. Y. Gong.

Z. Wang, W. Liu, and C. Qian are with Tsinghua National Laboratory for Information Science and Technology, Department of Electronic Engineering, Tsinghua University, Beijing 100084, China (e-mail: zcwang@tsinghua.edu.cn; lwd15@mails.tsinghua.edu.cn; qianc10@mails.tsinghua.edu.cn).

S. Chen is with the Department of Electronics and Computer Science, University of Southampton, Southampton SO17 1BJ, U.K., and also with King Abdulaziz University, Jeddah 21589, Saudi Arabia (e-mail: sqc@ecs.soton.ac.uk).

L. Hanzo is with the Department of Electronics and Computer Science, University of Southampton, Southampton SO17 1BJ, U.K. (e-mail: lh@ecs.soton.ac.uk).

Color versions of one or more of the figures in this paper are available online at http://ieeexplore.ieee.org.

Digital Object Identifier 10.1109/TVT.2016.2622009

II. System Model and Kronecker Structure

For simplicity of illustration, let us consider the single-cell scenario supporting K single-antenna-aided users, noting that our scheme is equally applicable to multicell scenarios. The BS employs a URA having M_y and M_x antennas in the elevation and azimuth domains, respectively. The number of antennas at the BS is, thus, $M = M_y M_x$. Let D_y and D_x be the antenna spacings in the elevation and azimuth domains, respectively. We assume that $D_x = D_y = D$. Let us furthermore denote the downlink channel matrix between the BS and the kth user by $\mathbf{H}_k = \left[\mathbf{h}_{k,1}\ \mathbf{h}_{k,2}\ \cdots\ \mathbf{h}_{k,M_y}\right]^T \in \mathbb{C}^{M_y \times M_x}$, where $\mathbf{h}_{k,l}^T \in \mathbb{C}^{1\times M_x}$ is the lth row of $\mathbf{H}_k$ and $(\,)^T$ denotes the transpose operator. An equivalent vectorial form of $\mathbf{H}_k$ is $\mathbf{h}_{\mathrm{vec},k} = \left[\mathbf{h}_{k,1}^T\ \mathbf{h}_{k,2}^T\ \cdots\ \mathbf{h}_{k,M_y}^T\right]^T \in \mathbb{C}^{(M_x M_y)\times 1}$. Denote $\mathbf{x} = \left[x_1\ x_2\ \cdots\ x_K\right]^T$ with $E\{\mathbf{x}\mathbf{x}^H\} = \mathbf{I}_K$, which contains the symbols transmitted by the BS to the K users, where $(\,)^H$ is the conjugate transpose operator and $E\{\,\}$ denotes the expectation. The received signal vector $\mathbf{r} = \left[r_1\ r_2\ \cdots\ r_K\right]^T \in \mathbb{C}^{K\times 1}$ by the K users can be expressed as

$$\mathbf{r} = \mathbf{H}_{\mathrm{vec}}\mathbf{W}_{\mathrm{vec}}\mathbf{x} + \mathbf{n} \tag{1}$$

where $\mathbf{n} = \left[n_1\ n_2\ \cdots\ n_K\right]^T \in \mathbb{C}^{K\times 1}$ is the additive white Gaussian noise (AWGN) vector experienced in the downlink, and $\mathbf{H}_{\mathrm{vec}} = \left[\mathbf{h}_{\mathrm{vec},1}\,\mathbf{h}_{\mathrm{vec},2}\cdots\mathbf{h}_{\mathrm{vec},K}\right]^T \in \mathbb{C}^{K\times(M_x M_y)}$ is the downlink channel matrix between the BS and the K users, while $\mathbf{W}_{\mathrm{vec}} = \left[\mathbf{w}_{\mathrm{vec},1}\,\mathbf{w}_{\mathrm{vec},2}\cdots\mathbf{w}_{\mathrm{vec},K}\right] \in \mathbb{C}^{(M_x M_y)\times K}$ is the precoding matrix associated, with $\mathbf{w}_{\mathrm{vec},k} \in \mathbb{C}^{(M_x M_y)\times 1}$ being the TPC vector for the kth user. Hence, the received signal of the kth user is given by

$$r_k = \mathbf{h}_{\mathrm{vec},k}^T\mathbf{w}_{\mathrm{vec},k}x_k + \sum_{k'\neq k}\mathbf{h}_{\mathrm{vec},k}^T\mathbf{w}_{\mathrm{vec},k'}x_{k'} + n_k. \tag{2}$$

The second term on the right-hand side of (2) represents the interuser interference, also known as intracell interference, and $\mathbf{W}_{\mathrm{vec}}$ is designed to eliminate this interference or to make it negligibly small. Note that in a multicell environment, there will also be an intercell interference component in r_k, and it becomes vital to ensure that the matrix $\mathbf{W}_{\mathrm{vec}}$ reduces this intercell interference.

We consider the following narrow-band multipath channel model [14]

$$\mathbf{H}_k = \sum_{p=1}^{P}\mathbf{H}_k^p \tag{3}$$

where P is the number of paths, and $\mathbf{H}_k^p \in \mathbb{C}^{M_y\times M_x}$ is the channel matrix of the pth path. The element at the lth row and mth column of $\mathbf{H}_k^p$ is given by [11]

$$\begin{aligned} h_k^{m,l,p} &= \rho_k^p e^{-j2\pi\frac{D}{\lambda}\left((m-1)\cos\theta_k^p\cos\beta_k^p + (l-1)\sin\beta_k^p\right)} \\ &= \rho_k^p e^{-j2\pi\frac{(m-1)D}{\lambda}\cos\theta_k^p\cos\beta_k^p} e^{-j2\pi\frac{(l-1)D}{\lambda}\sin\beta_k^p} \\ &= \rho_k^p h_{a,k}^{m,p} h_{e,k}^{l,p} \end{aligned} \tag{4}$$

where λ denotes the wavelength, θ_k^p is the angle-of-arrival in the azimuth domain (A-AOA), β_k^p is the angle-of-arrival in the elevation domain (E-AOA), and ρ_k^p is the large-scale fading coefficient of the pth path, while $h_{a,k}^{m,p} = e^{-j2\pi\frac{(m-1)D}{\lambda}\cos\theta_k^p\cos\beta_k^p}$ and $h_{e,k}^{l,p} = e^{-j2\pi\frac{(l-1)D}{\lambda}\sin\beta_k^p}$ denote the azimuth and elevation components of $h_k^{m,l,p}$, respectively. Observe from (4) that $\mathbf{H}_k^p$ has the following Kronecker structure:

$$\mathbf{H}_k^p = \rho_k^p\left(\mathbf{h}_{a,k}^p\right)^T \otimes \mathbf{h}_{e,k}^p \tag{5}$$

in which $\otimes$ denotes the Kronecker product operator

$$\mathbf{h}_{a,k}^p = \left[1\, h_{a,k}^{1,p}\cdots h_{a,k}^{m,p}\cdots h_{a,k}^{(M_x-1),p}\right]^T \tag{6}$$

and

$$\mathbf{h}_{e,k}^p = \left[1\, h_{e,k}^{1,p}\cdots h_{e,k}^{l,p}\cdots h_{e,k}^{(M_y-1),p}\right]^T \tag{7}$$

are the azimuth- and elevation-domain steering vectors, respectively. The overall channel matrix can then be written as

$$\mathbf{H}_k = \sum_{p=1}^{P}\rho_k^p\left(\mathbf{h}_{a,k}^p\right)^T \otimes \mathbf{h}_{e,k}^p. \tag{8}$$

Under the assumption that the angular spread of E-AOA is small, which is reasonable since compared to the height of the BS, the distance between the BS and the user is high, we have $\mathbf{h}_{e,k}^p \approx \mathbf{h}_{e,k}$ for $1 \le p \le P$, with $\mathbf{h}_{e,k}$ being the approximated elevation-domain steering vector. Thus, $\mathbf{H}_k$ can be approximated by

$$\mathbf{H}_k \approx \left(\sum_{p=1}^{P}\rho_k^p\left(\mathbf{h}_{a,k}^p\right)^T\right) \otimes \mathbf{h}_{e,k}. \tag{9}$$

The existing beamforming scheme [7] is based on the approximated elevation steering vector $\mathbf{h}_{e,k}$. This scheme first performs eigenbeamforming in the elevation domain and then performs TPC in the azimuth domain by exploiting the equivalent azimuth-domain steering vector obtained by eigenbeamforming. Let $\mathbf{R}_e = E\{\mathbf{h}_{e,k}\mathbf{h}_{e,k}^H\}$ be the correlation matrix in the elevation domain, which is subjected to eigendecomposition. The eigenvector corresponding to the largest eigenvalue of $\mathbf{R}_e$ is chosen as the beamforming vector. In fact, this approximation may not completely conform to some communication scenarios according to 3-D channel measurements results, which leads to some performance loss [15].

On the other hand, the conventional full TPC scheme [2], [3] directly calculates the precoding matrix based on the channel matrix $\mathbf{H}_k$ or its vectorial form of $\mathbf{h}_{\mathrm{vec},k}$ and does not exploit the Kronecker structure of the channel matrix (8). As a result, the computational complexity of this conventional full TPC scheme is high, on the order of $M_x M_y$, which is denoted as $\mathsf{O}(M_x M_y)$. This full TPC scheme is known to be efficient in terms of combating the interuser interference, and it is optimal in the single-cell environment. However, in a multicell scenario subjected to strong intercell interference, the achievable performance of this full TPC scheme may actually be worse than that of the conventional beamforming scheme, as will be shown later in our simulation study.

III. Two-Dimensional Precoding Scheme

This section details our proposed 2-D precoding scheme conceived for 3-D MMIMOs, which is capable of eliminating the interuser interference, while maintaining a significantly lower computational complexity than the existing full precoding scheme.

A. Proposed Scheme

The idea is to perform elevation- and azimuth-domain TPC separately by exploiting the Kronecker structure of the approximate channel matrix (9). First, the approximated elevation-domain channel vector $\overline{\mathbf{h}}_{e,k}$ is obtained from the estimation of the coefficients between the kth user and any column of the 2-D antenna array. Then, we calculate the elevation-domain precoding vector based on $\overline{\mathbf{h}}_{e,k}$. For the generic

TABLE I
PROCEDURE OF PROPOSED 2-D PRECODING SCHEME FOR 3-D MIMO

Parameters	The number of users per cell, K, and the dimension of URA, $M_y \times M_x$
Inputs	The 3-D channel matrices $\mathbf{H}_k$, $1 \le k \le K$
Step 1	Obtain the approximated elevation steering vector $\overline{\mathbf{h}}_{e,k}$ from the 3-D channel matrix (9)
Step 2	2.1: Construct the elevation channel matrix $\overline{\mathbf{H}}_e$ 2.2: Perform the ZF precoding on $\overline{\mathbf{H}}_e$ to obtain the elevation precoding channel matrix $\mathbf{W}_e$
Step 3	Obtain the equivalent azimuth steering vector $\mathbf{h}_{a,k}^{\mathrm{eq}}$
Step 4	4.1: Construct the azimuth channel matrix $\overline{\mathbf{H}}_a^{\mathrm{eq}}$ 4.2: Perform the ZF precoding on $\overline{\mathbf{H}}_a^{\mathrm{eq}}$ to obtain the azimuth precoding channel matrix $\mathbf{W}_a$
Step 5	Calculate the overall precoding matrix $\mathbf{W}_k$ for the kth user using Kronecker product

multiuser scenario, the elevation-domain channel matrix is constructed as

$$\overline{\mathbf{H}}_e = \left[\overline{\mathbf{h}}_{e,1}\ \overline{\mathbf{h}}_{e,2}\ \cdots\ \overline{\mathbf{h}}_{e,K}\right]^T \in \mathbb{C}^{K\times M_y}. \tag{10}$$

When the zero-forcing (ZF) precoding algorithm is used, the elevation-domain TPC matrix is calculated as

$$\mathbf{W}_e = \overline{\mathbf{H}}_e^H \left(\overline{\mathbf{H}}_e \overline{\mathbf{H}}_e^H\right)^{-1} \mathbf{\Gamma}_e \in \mathbb{C}^{M_y\times K} \tag{11}$$

where $\mathbf{\Gamma}_e = \mathrm{diag}\{\gamma_{e,1}, \gamma_{e,2}, \ldots, \gamma_{e,K}\} \in \mathbb{C}^{K\times K}$ is a diagonal matrix for the normalization of the precoding matrix, and $\mathbf{W}_e = \left[\mathbf{w}_{e,1}\, \mathbf{w}_{e,2} \cdots \mathbf{w}_{e,K}\right]$, with $\mathbf{w}_{e,k} \in \mathbb{C}^{M_y\times 1}$ being the TPC vector of the kth user.

Then, the equivalent azimuth-domain channel vector is obtained based on $\mathbf{H}_k$ and $\mathbf{w}_{e,k}$. Specifically, the equivalent azimuth-domain channel vector $\mathbf{h}_{a,k}^{\mathrm{eq}} \in \mathbb{C}^{M_x\times 1}$ of the kth user is given by

$$\mathbf{h}_{a,k}^{\mathrm{eq}} = \mathbf{H}_k^T \mathbf{w}_{e,k}. \tag{12}$$

Next, the azimuth-domain TPC vector is calculated based on $\mathbf{h}_{a,k}^{\mathrm{eq}}$. Applying the ZF TPC algorithm to the equivalent azimuth-domain channel matrix

$$\mathbf{H}_a^{\mathrm{eq}} = \left[\mathbf{h}_{a,1}^{\mathrm{eq}}\ \mathbf{h}_{a,2}^{\mathrm{eq}}\ \cdots\ \mathbf{h}_{a,K}^{\mathrm{eq}}\right]^T \in \mathbb{C}^{K\times M_x} \tag{13}$$

yields the azimuth-domain TPC matrix

$$\mathbf{W}_a = \left(\mathbf{H}_a^{\mathrm{eq}}\right)^H \left(\mathbf{H}_a^{\mathrm{eq}} \left(\mathbf{H}_a^{\mathrm{eq}}\right)^H\right)^{-1} \mathbf{\Gamma}_a \in \mathbb{C}^{M_x\times K} \tag{14}$$

where $\mathbf{\Gamma}_a = \mathrm{diag}\{\gamma_{a,1}, \gamma_{a,2}, \ldots, \gamma_{a,K}\} \in \mathbb{C}^{K\times K}$ is a diagonal matrix for the normalization of the precoding matrix, and $\mathbf{W}_a = \left[\mathbf{w}_{a,1}\, \mathbf{w}_{a,2} \cdots \mathbf{w}_{a,K}\right]$, with $\mathbf{w}_{a,k} \in \mathbb{C}^{M_x\times 1}$ being the azimuth precoding vector for the kth user.

Finally, the overall TPC matrix of the kth user is constructed as

$$\mathbf{W}_k = \mathbf{w}_{a,k}^T \otimes \mathbf{w}_{e,k} \in \mathbb{C}^{M_y\times M_x}. \tag{15}$$

Table I summarizes the procedure of this 2-D TPC scheme. Based on the TPC matrix $\mathbf{W}_k$ of (15), the received signal r_k of the kth user will not be contaminated by the other users in the same cell, and our 2-D TPC algorithm has a low complexity. We justify the efficiency of our proposal and its low complexity in the next two subsections.

B. Interuser Interference Reduction

We prove that based on the TPC matrix $\mathbf{W}_k$ (15), the interuser interference imposed on the received signal r_k can be eliminated in the single-cell scenario when encountering the ideal MIMO channel of (9), i.e., $\mathbf{h}_{e,k}^p = \mathbf{h}_{e,k}$ for $1 \le p \le P$. Let $H_k^{(l,m)}$ and $W_k^{(l,m)}$ be the lth row and mth column elements of $\mathbf{H}_k$ and $\mathbf{W}_k$, respectively. Furthermore, let us define the operator $\oplus$ as the "inner product" of two matrices according to

$$\mathbf{H}_k \oplus \mathbf{W}_k = \sum_{m=0}^{M_x-1} \sum_{l=0}^{M_y-1} H_k^{(l,m)} W_k^{(l,m)}. \tag{16}$$

Let $w_{a,k}^m$ be the mth term of the azimuth TPC vector $\mathbf{w}_{a,k}$. Bearing in mind $\mathbf{H}_k$ of (9) and $\mathbf{W}_k$ of (15), we have

$$\begin{aligned}\mathbf{H}_k \oplus \mathbf{W}_k &= \sum_{m=0}^{M_x-1} \left(\sum_{p=1}^{P} \left(\rho_k^p h_{a,k}^{m,p} \mathbf{h}_{e,k}^T\right)\left(w_{a,k}^m \mathbf{w}_{e,k}\right)\right) \\ &= \mathbf{h}_{e,k}^T \mathbf{w}_{e,k} \sum_{p=1}^{P} \rho_k^p \sum_{m=0}^{M_x-1} w_{a,k}^m h_{a,k}^{m,p} \\ &= \gamma_{e,k} \sum_{p=1}^{P} \rho_k^p \left(\mathbf{h}_{a,k}^p\right)^T \mathbf{w}_{a,k}. \end{aligned} \tag{17}$$

Then, substituting $\mathbf{H}_k$ of (9) into (12) yields

$$\begin{aligned}\mathbf{h}_{a,k}^{\mathrm{eq}} &= \mathbf{h}_{e,k}^T \otimes \left(\sum_{p=1}^{P} \rho_k^p \mathbf{h}_{a,k}^p\right) \mathbf{w}_{e,k} \\ &= \mathbf{h}_{e,k}^T \mathbf{w}_{e,k} \sum_{p=1}^{P} \rho_k^p \mathbf{h}_{a,k}^p = \gamma_{e,k} \sum_{p=1}^{P} \rho_k^p \mathbf{h}_{a,k}^p. \end{aligned} \tag{18}$$

Hence, $\mathbf{H}_k \oplus \mathbf{W}_k = \left(\mathbf{h}_{a,k}^{\mathrm{eq}}\right)^T \mathbf{w}_{a,k} = \gamma_{a,k}$. The computation of $\mathbf{H}_k \oplus \mathbf{W}_{k'}$ for $k' \ne k$ is similar, and we have $\mathbf{H}_k \oplus \mathbf{W}_{k'} = \mathbf{h}_{e,k}^T \mathbf{w}_{e,k'}$. Since $\mathbf{h}_{e,k}^T \mathbf{w}_{e,k'} = 0$ when $k' \ne k$, we have

$$\mathbf{H}_k \oplus \mathbf{W}_{k'} = \begin{cases} \gamma_{a,k}, & k' = k \\ 0, & k' \ne k. \end{cases} \tag{19}$$

One the other hand, $\mathbf{h}_{\mathrm{vec},k}^T \mathbf{w}_{\mathrm{vec},k'}$ in (2) is given by

$$\mathbf{h}_{\mathrm{vec},k}^T \mathbf{w}_{\mathrm{vec},k'} = \mathbf{H}_k \oplus \mathbf{W}_{k'}, \quad 1 \le k' \le K. \tag{20}$$

Therefore, the desired signal term in (2) is $\gamma_{a,k} x_k$, and the interuser interference term becomes zero. Thus, the proposed scheme completely eliminates the interuser interference, despite having only a limited number of antennas in the elevation domain.

C. Complexity Analysis

Compared to the conventional multiplexing scheme [2], [3], which carries out full TPC based on the channel matrix $\mathbf{H}_k$ or its vectorial form $\mathbf{h}_{\mathrm{vec},k}$ directly, our 2-D TPC scheme has a significantly lower complexity. Specifically, it replaces the $M = M_x M_y$-dimensional matrix operations by M_x-dimensional and M_y-dimensional matrix operations by exploiting the Kronecker structure of the channel matrix. It is widely recognized that given a certain number of users K, the computational complexity of the TPC is dominated by the matrix multiplication, which is proportional to the matrix dimension involved. As a direct consequence of exploiting the Kronecker structure of the channel matrix, the $\mathsf{O}\left(M_x M_y\right)$ complexity required by the conventional full TPC scheme is reduced to $\mathsf{O}\left(M_x + M_y\right)$ in our 2-D TPC scheme, which is significant, especially for massive MIMO schemes.

D. Multicell Scenario

As pointed out previously, our proposed 2-D TPC scheme is equally applicable to the multicell scenario. Let L be the number of cells and K be the number of users per cell, which are served during the same time/frequency resource. Let us denote the downlink channel matrix between the BS of the s-cell and the kth user in the qth cell by $\mathbf{H}_{k,q,s} \in \mathbb{C}^{M_y \times M_x}$. The following P-path narrow-band multipath channel model is considered [14]

$$\mathbf{H}_{k,q,s} = \sum_{p=1}^{P} \mathbf{H}_{k,q,s}^{p} \tag{21}$$

where $\mathbf{H}_{k,q,s}^{p}$ denotes the pth path component of the channel matrix. The element at the lth row and mth column of $\mathbf{H}_{k,q,s}^{p}$ is given by

$$h_{k,q,s}^{m,l,p} = \rho_{k,q,s}^{p} e^{-j2\pi \frac{D}{\lambda}\left((m-1)\cos\theta_{k,q,s}^{p}\cos\beta_{k,q,s}^{p} + (l-1)\sin\beta_{k,q,s}^{p}\right)} \tag{22}$$

where $\theta_{k,q,s}^{p}$ and $\beta_{k,q,s}^{p}$ are the A-AOA and E-AOA of the pth path, respectively, and the large-scale fading coefficient $\rho_{k,q,s}^{p}$ is given by

$$\rho_{k,q,s}^{p} = \frac{z_{k,q,s}^{p}}{(d_{k,q,s})^{\alpha}} \tag{23}$$

in which $d_{k,q,s}$ denotes the distance between the BS of the s-cell and the kth user in the qth cell, α is the path-loss exponent, and $z_{k,q,s}^{p}$ is the shadow-fading coefficient that follows the log-normal distribution with a variance of σ_z^2.

Under the condition that there are K orthogonal pilots, which are reused in every cell [16], the channel estimation at the BS of the qth cell is formulated as

$$\widehat{\mathbf{H}}_{k,q,q} = \mathbf{H}_{k,q,q} + \sum_{s \neq q} \mathbf{H}_{k,q,s} \tag{24}$$

in the absence of AWGN. The BS utilizes the estimate $\widehat{\mathbf{H}}_{k,q,q}$ to obtain the TPC matrix and transmits the downlink data. The ubiquitous pilot-contamination degrades the channel estimate of (24), which imposes intercell interference and degrades the overall performance. The following analysis will illuminate how the 2-D TPC deals with this intercell interference in order to further improve the overall performance in multicell scenarios.

When taking the intercell interference into consideration, the elevation channel matrix of (10) is rewritten as

$$\widehat{\overline{\mathbf{H}}}_{e} = \left[\widehat{\overline{\mathbf{h}}}_{e,1},\ \widehat{\overline{\mathbf{h}}}_{e,2}\ \cdots\ \widehat{\overline{\mathbf{h}}}_{e,K}\right]^{T} \in \mathbb{C}^{K \times M_y} \tag{25}$$

where $\widehat{\overline{\mathbf{h}}}_{e,k} \in \mathbb{C}^{M_y \times 1} = \overline{\mathbf{h}}_{e,k} + \mathbf{h}_{e,k,i}$ denotes the contaminated elevation channel vector for the kth user. Thus, $\widehat{\overline{\mathbf{H}}}_{e}$ can be simply decomposed into two parts as follows:

$$\widehat{\overline{\mathbf{H}}}_{e} = \overline{\mathbf{H}}_{e} + \mathbf{H}_{i} \tag{26}$$

where $\mathbf{H}_i$ indicates the intercell interference. Then, the elevation precoder generated from (11) is rewritten as $\widehat{\overline{\mathbf{W}}}_{e} = \widehat{\overline{\mathbf{H}}}_{e}^{H}\left(\widehat{\overline{\mathbf{H}}}_{e}\widehat{\overline{\mathbf{H}}}_{e}^{H}\right)^{-1}\widehat{\mathbf{\Gamma}}_{e} \in \mathbb{C}^{M_y \times K}$. Upon invoking the elevation precoder, we can obtain the equivalent downlink elevation channel $\mathbf{G}_e = \overline{\mathbf{H}}_{e}\widehat{\overline{\mathbf{W}}}_{e} \in \mathbb{C}^{K \times K}$, which is formulated as follows:

$$\begin{aligned}\mathbf{G}_e &= \overline{\mathbf{H}}_{e}(\overline{\mathbf{H}}_{e} + \mathbf{H}_{i})^{H}\left((\overline{\mathbf{H}}_{e} + \mathbf{H}_{i})(\overline{\mathbf{H}}_{e} + \mathbf{H}_{i})^{H}\right)^{-1}\widehat{\mathbf{\Gamma}}_{e} \\ &= (\overline{\mathbf{H}}_{e}\overline{\mathbf{H}}_{e}^{H} + \overline{\mathbf{H}}_{e}\mathbf{H}_{i}^{H})(\overline{\mathbf{H}}_{e}\overline{\mathbf{H}}_{e}^{H} + \overline{\mathbf{H}}_{e}\mathbf{H}_{i}^{H} \\ &\quad + \mathbf{H}_{i}\overline{\mathbf{H}}_{e}^{H} + \mathbf{H}_{i}\mathbf{H}_{i}^{H})^{-1}\widehat{\mathbf{\Gamma}}_{e}.\end{aligned} \tag{27}$$

TABLE II
PARAMETERS OF THE SIMULATED SINGLE-CELL MULTIUSER SYSTEM

Number of users per cell K	8
Cell radius	250 m
Height of BS	35 m
Path-loss exponent α	3.5
Variance of shadow fading σ_z^2	8 dB
Antenna spacing D	$\lambda/2$
Number of paths P	10
Angle spread of A-AOA δ_θ	180°
Angle spread of E-AOA δ_β	2.5°

The two parts of $\widehat{\overline{\mathbf{h}}}_{e,k}$ can be formulated in detail as $\overline{\mathbf{h}}_{e,k}(\{\beta_{k,c}\})$ and $\mathbf{h}_{e,k,i}(\{\beta_{k,i}\})$, where $\{\beta_{k,c}\}$ and $\{\beta_{k,i}\}$ represent the sets of E-AOAs for the signals impinging from the center cell and from the other cells, respectively. It is critical that the E-AOAs of the rays impinging from the other cells are much smaller at the users than those of the center cell, which implies that the signals will not overlap in the elevation domain. This property can be formulated as

$$\begin{aligned}&\{\beta_{k,c}\} \cap \{\beta_{k,i}\} = \varnothing \\ &\forall \beta_1 \in \{\beta_{k,c}\}, \beta_2 \in \{\beta_{k,i}\}, \beta_1 > \beta_2.\end{aligned} \tag{28}$$

Thus, exploiting the associated asymptotic property, we have

$$\begin{aligned}\lim_{M_y \to \infty} \overline{\mathbf{h}}_{e,k}^{H}\mathbf{h}_{e,k,i} &= 0 \\ \lim_{M_y \to \infty} \overline{\mathbf{H}}_{e}\mathbf{H}_{i}^{H} &= \mathbf{0}_K \\ \lim_{M_y \to \infty} \mathbf{H}_{i}\overline{\mathbf{H}}_{e}^{H} &= \mathbf{0}_K.\end{aligned} \tag{29}$$

Then, the equivalent channel $\mathbf{G}_e$ can be approximated as

$$\mathbf{G}_e \approx \overline{\mathbf{H}}_{e}\overline{\mathbf{H}}_{e}^{H}(\overline{\mathbf{H}}_{e}\overline{\mathbf{H}}_{e}^{H} + \mathbf{H}_{i}\mathbf{H}_{i}^{H})^{-1}\widehat{\mathbf{\Gamma}}_{e} \tag{30}$$

where $\mathbf{H}_i\mathbf{H}_i^H$ remains nonzero, which indicates that although the intercell interference signals cannot be completely eliminated, they can be considerably reduced. Therefore, we can see that $\mathbf{G}_e \approx \widehat{\mathbf{\Gamma}}_e$, and the intercell interference is reduced in the elevation domain, which considerably improves the overall performance in our multicell scenario in comparison to the conventional TPC algorithms. It is worth pointing out that in combination with the classic downtilting or beamforming, the intercell interference imposed by the pilot reuse can be further reduced [6].

IV. PERFORMANCE EVALUATION

Our numerical results provided in this section reveal the superiority of our proposal. The single-cell scenario is considered in detail, complemented by the portrayal of the intercell interference reduction attained in a multicell scenario.

A. Single-Cell Simulations

The parameters of the simulated single-cell multiuser systems are listed in Table II. The BS is located in the center, while the users are randomly dispersed. In the azimuth domain, the users' A-AOA is uniformly distributed in $\left[\theta_c - \delta_\theta/2,\ \theta_c + \delta_\theta/2\right]$, with a mean of θ_c and an angular spread of δ_θ. Similarly, in the elevation domain, the users' E-AOA is uniformly distributed in $\left[\beta_c - \delta_\beta/2,\ \beta_c + \delta_\beta/2\right]$, with a mean of β_c and an angular spread of δ_β. The URA is set to be square,

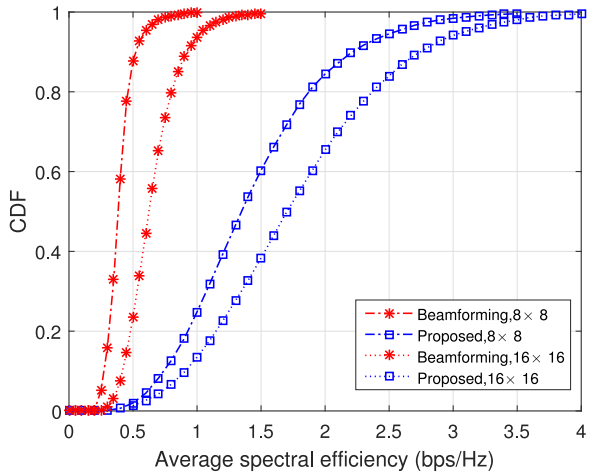

Fig. 1. CDF comparison of downlink average spectral efficiency for the proposed scheme and conventional beamforming scheme in Case 1. 8×8 and 16×16 URA are adopted.

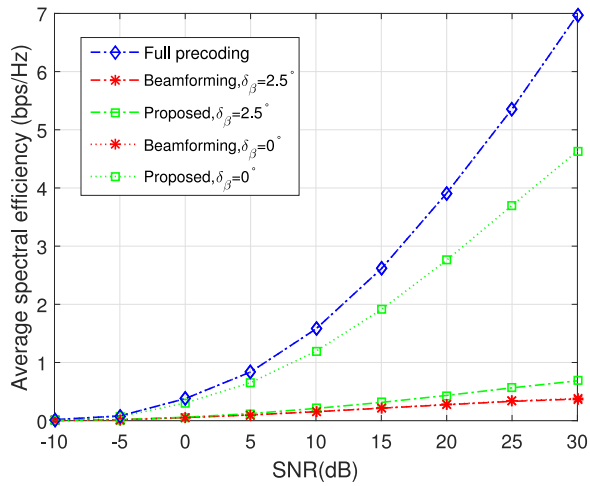

Fig. 2. Comparison of downlink average spectral efficiency for the proposed scheme, conventional beamforming scheme, and full-precoding in Case 2. 8×8 URA is adopted.

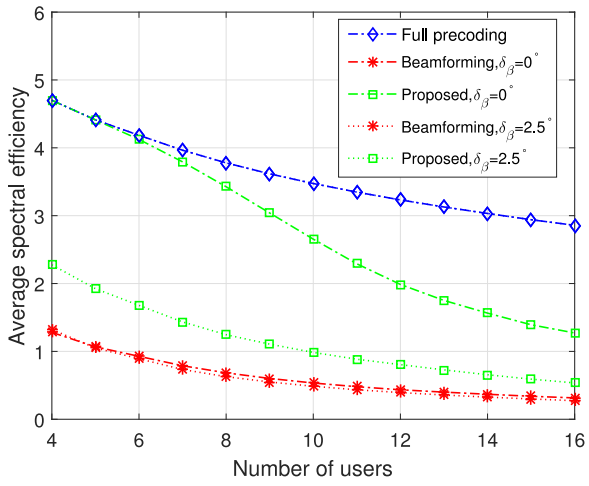

Fig. 3. Comparison of downlink average spectral efficiency for the proposed scheme, conventional beamforming scheme, and full-precoding in Case 3 with different number of users K. 16×16 URA is adopted and SNR $= 20$ dB.

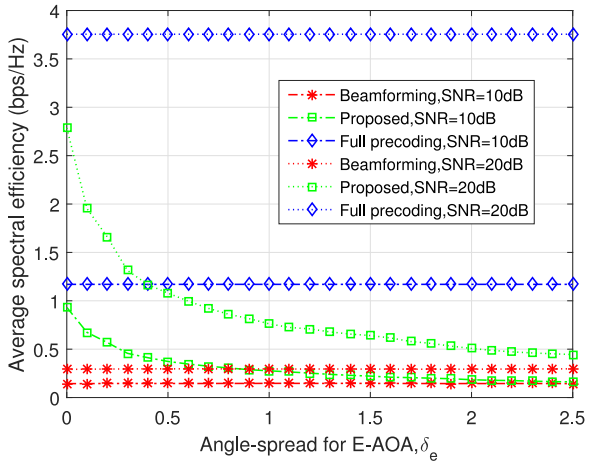

Fig. 4. Comparison of downlink average spectral efficiency for the proposed scheme, conventional beamforming scheme, and full-precoding in Case 4 with different angle spreads in elevation domain. 8×8 URA is adopted.

i.e., $M_x = M_y = \sqrt{M}$. We consider downlink data transmission, and the proposed 2-D TPC scheme is compared both to the existing conventional beamforming scheme [7], [8] and to the conventional full TPC scheme [2], [3].

1) Case 1: The cumulative distribution function (CDF) of the downlink average spectral efficiency evaluated in the absence of noise is shown in Fig. 1. The full-precoding algorithm is not included here because of its infinite spectral efficiency in the idealized noise-free scenario. Observe in Fig. 1 that the 2-D TPC scheme substantially outperforms the conventional beamforming scheme. As the number of antennas per dimension increases, the spectral efficiency of our 2-D precoding scheme improves more significantly since the TPC of the elevation domain becomes more accurate.

2) Case 2: In this context, the average downlink spectral efficiency achieved at different signal-to-noise ratios (SNRs) (in dB) is presented. Naturally, the full-precoding performs best in the single-cell scenario, since it substantially reduced the interuser interference, albeit at a high implementation complexity. The other two schemes exploited the Kronecker product structure of the 3-D channel matrix, where a somewhat higher interuser interference persisted.

The derivation of our proposed 2-D TPC scheme relies on the approximation of all the elevation-domain channel vectors $\mathbf{h}_{e,k}^{p}, 1 \leq p \leq P$ by the same approximated elevation-domain channel vector $\mathbf{h}_{e,k}$. The smaller the angular spread δ_β of E-AOA, the more accurate this approximation becomes. When we have $\delta_\beta = 0$, the approximation becomes the exact solution. Observe in Fig. 2 that compared to the case of $\delta_\beta = 2.5°$, our proposal performs much better with $\delta_\beta = 0°$, which approaches the performance of the full-precoding aided scheme.

3) Case 3: Observe from Fig. 3 that as the number of users increases, the average downlink spectral efficiency reduces for all the schemes due to the higher interuser interference. Meanwhile, although the performance gap between the proposed 2-D TPC algorithm and the conventional beamforming decreases with large number of users, the proposed 2-D TPC algorithm still outperforms conventional beamforming scheme—regardless of the number of users—owing to its superiority in reducing the interuser interference.

4) Case 4: Fig. 4 shows our performance comparison of the three algorithms under different angular spreads in the elevation

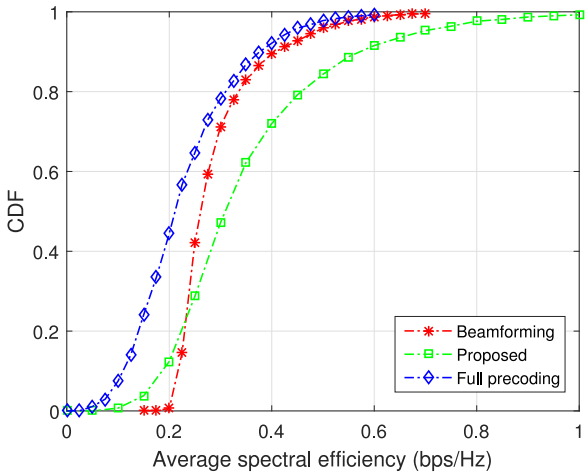

Fig. 5. CDF comparison of downlink average spectral efficiency for the proposed scheme, conventional beamforming scheme, and full-precoding in a multicell scenario. 8×8 URA is adopted.

domain. As δ_β increases from 0° to 2.5°, the performance of the 2-D TPC rapidly erodes due to the inaccuracy of the channel approximation in the elevation domain, which has been characterized in cases 2 and 3. However, the conventional beamforming scheme is insensitive to δ_β, while the performance of the full-precoding scheme is independent of δ_β. In most scenarios, δ_β is small enough to ensure a high performance for our proposal [15].

B. Multicell Simulation

The noise-free multicell scenario is characterized in this subsection to demonstrate the superiority of our 2-D TPC in reducing the intercell interference. $L = 7$ cells are considered, and the other parameters are the same as in the single-cell scenario. Fig. 5 compares the downlink spectral efficiency achieved by the proposed scheme to those of the conventional beamforming scheme and of the full TPC scheme, where it can be seen that our 2-D TPC scheme substantially outperforms the existing beamforming scheme. Furthermore, it can be observed from Fig. 5 that the performance of the existing full TPC scheme is actually worse than that of the existing beamforming scheme in this hostile intercell interference environment. Thus, our proposed 2-D precoding scheme not only dramatically outperforms the conventional full TPC scheme but has a much lower computational complexity as well.

V. Conclusion

A novel 2-D TPC scheme has been proposed for 3-D massive MIMO, which performs elevation-domain precoding and azimuth-domain precoding separately by exploiting the Kronecker structure of the 3-D MIMO channel. Unlike the conventional beamforming scheme, which fails to completely eliminate the intracell or interuser interference with the aid of a finite number of antennasin the elevation domain, our proposed scheme fully exploits the degrees of freedom introduced by the elevation-domain antennas for eliminating the interuser interference. Compared to the existing full TPC scheme, which does not exploit the Kronecker structure of the 3-D MIMO channel, our 2-D TPC scheme offers a much lower complexity. Our simulation results have verified the superior performance of our proposed scheme over the existing beamforming and full precoding schemes in severe intercell interference environments.

References

[1] E. G. Larsson, O. Edfors, F. Tufvesson, and T. L. Marzetta, "Massive MIMO for next generation wireless systems," *IEEE Commun. Mag.*, vol. 52, no. 2, pp. 186–195, Feb. 2014.

[2] F. Rusek *et al.*, "Scaling up MIMO: Opportunities and challenges with very large arrays," *IEEE Signal Process. Mag.*, vol. 30, no. 1, pp. 40–60, Jan. 2013.

[3] T. L. Marzetta, "Noncooperative cellular wireless with unlimited numbers of base station antennas," *IEEE Trans. Wireless Commun.*, vol. 9, no. 11, pp. 3590–3600, Nov. 2010.

[4] H. Q. Ngo, E. G. Larsson, and T. L. Marzetta, "Energy and spectral efficiency of very large multiuser MIMO systems," *IEEE Trans. Commun.*, vol. 61, no. 4, pp. 1436–1449, Apr. 2013.

[5] Y.-H. Nam *et al.*, "Full-dimension MIMO (FD-MIMO) for next generation cellular technology," *IEEE Commun. Mag.*, vol. 51, no. 6 pp. 172–179, Jun. 2013.

[6] S. Akoum and J. Acharya, "Full-dimensional MIMO for future cellular networks," in *Proc. IEEE Radio Wireless Symp.*, Newport Beach, CA, USA, Jan. 19–23, 2014, pp. 1–3.

[7] Y. Song, S. Nagata, H. Jiang, and L. Chen, "CSI-RS design for 3D MIMO in future LTE-advanced," in *Proc. IEEE Int. Conf. Commun.*, Sydney, Australia, Jun. 10–14, 2014, pp. 5101–5106.

[8] A. Alkhateeby, G. Leusz, and R. W. Heath Jr.,, "Multi-layer precoding for full-dimensional massive MIMO systems," in *Proc. 48th Asilomar Conf. Signals, Syst. Comput.*, Nov. 2–5, 2014, pp. 815–819.

[9] L. You, X. Gao, X.-G. Xia, N. Ma, and Y. Peng, "Massive MIMO transmission with pilot reuse in single cell," in *Proc. IEEE Int. Conf. Commun.*, Sydney, Australia, Jun. 10–14, 2014, pp. 4794–4799.

[10] F. W. Vook, E. Visotsky, T. A. Thomas, and B. Mondal, "Product codebook feedback for massive MIMO with cross-polarized 2D antenna arrays," in *Proc. 25th IEEE Annu. Int. Symp. Pers., Indoor, Mobile Radio Commun.*, Washington, DC, USA, Sep. 2–5, 2014, pp. 502–506.

[11] R1-150713, Samsung, "Discussion on FD-MIMO Codebook Enhancements," 3GPP TSG RAN WG1 #80 (Athens, Greece), Feb. 9–13, 2015.

[12] R1-150516, NVIDIA, "Performance of Kronecker-based CSI feedback for EBF/FD-MIMO," 3GPP TSG RAN WG1 #80 (Athens, Greece), Feb. 9–13, 2015.

[13] Y.-H. Nam, M. S. Rahman, Y. Li, and J.-Y. Seol, "Full dimension MIMO for LTE-Advanced and 5G," in *Proc. ITA Workshop*, San Diego, CA, USA, Feb. 1–6, 2015, pp. 1–6.

[14] A. Kammoun, H. Khanfir, Z. Altman, M. Debbah, and M. Kammoun, "Preliminary results on 3D channel modeling: From theory to standardization," *IEEE J. Sel. Areas Commun.*, vol. 32, no. 6, pp. 1219–1229, Jun. 2014.

[15] J. Wang, R. Zhang, W. Duan, S. X. Lu, and L. Cai, "Angular spread measurement and modeling for 3D MIMO in urban macrocellular radio channels," in *Proc. IEEE Int. Conf. Commun.*, Sydney, Australia, Jun. 10–14, 2014, pp. 20–25.

[16] A. Hu, T. Lv, H. Gao, Y. Lu, and E. Liu, "Pilot design for large-scale multi-cell multiuser MIMO systems," in *Proc. IEEE Int. Conf. Commun.*, Budapest, Hungry, Jun. 9–13, 2013, pp. 5381–5385.